IEEE Access
Multidisciplinary | Rapid Review | Open Access Journal

IEEE SYSTEMS, MAN AND CYBERNETICS SOCIETY SECTION

Received 8 February 2023, accepted 1 March 2023, date of publication 9 March 2023, date of current version 15 March 2023.

Digital Object Identifier 10.1109/ACCESS.2023.3254591

RESEARCH ARTICLE

Optimization Reinforced PID-Sliding Mode Controller for Rotary Inverted Pendulum

ARULMOZHI NAGARAJAN[1], (Member, IEEE), AND ARULDOSS ALBERT VICTOIRE[2], (Member, IEEE)

[1]Government College of Technology at Coimbatore, Coimbatore, Tamilnadu 641013, India
[2]Anna University Regional Campus at Coimbatore, Coimbatore, Tamilnadu 641046, India

Corresponding author: Arulmozhi Nagarajan (arulmozhi6@gct.ac.in)

ABSTRACT The control of a rotary inverted pendulum (RIP) is challenging because it is an underactuated, highly sensitive, and unsteady system. Sliding mode control (SMC) is a nonlinear control method with high-frequency switching control. Designing a proportional integral derivative (PID) controller for a RIP is challenging due to its nonlinearity and instability in open-loop characteristics. The primacy of the SMC over the PID is the stability of the closed-loop. Hybrid control of a PID-SMC controller can provide better performance because this technique demonstrates less chatter, higher precision, no oscillation, and adequate gain tuning. To achieve gain tuning, the PID and SMC parameters must be optimized. Thus, this paper proposed a congruently tuned control strategy (CTCS) to fine-tune the controller parameters. The proposed strategy uses an improved whale optimization algorithm (WOA), i.e., the modified Manhattan distance updated WOA (MMD-WOA) to identify effective coefficient values for the sliding surface to reduce tracking errors while reaching the desired position. The proposed CTCS for a RIP with the MMD-WOA was implemented, and the results are very promising.

INDEX TERMS Rotary inverted pendulum, congruently tuned control strategy, sliding mode control, optimization, stability criteria.

I. INTRODUCTION

In the control engineering field, the inverted pendulum (IP) is the most difficult system to control [1], [2]. IPs are highly nonlinear, underactuated, multivariable, and exhibit open-loop instability, and non-minimum phase. Currently, different types of IPs are available, and the most common are the linear, spherical, double, and rotary IPs. The rotary IP (RIP) is the most commonly investigated nonlinear system due to its static instability. A pendulum stabilization method has been proposed previously [3], [4] to improve the performance of the RIP. This method has been applied in various applications, e.g., position control, aerospace vehicle control, and robotics [5]. Due to their structural simplicity and sturdiness [6], [7], various tracking and stabilization control techniques, including linear control, nonlinear control, and self-learning control, are used. To maintain an erect pendulum position [4], [8], [9], complex control methods, e.g., full state feedback, proportional integral derivative (PID) control, and linear quadratic regulator (LQR) control, are employed to achieve the stability of the unstable RIP [10]. Friction forces in the joints of a nonlinear RIP can lead to steady-state errors within limited periods and reduce performance [11]. In addition, the sliding mode controller (SMC) is a unique and effective nonlinear control method due to its simple design and robustness [12], [13]. However, the SMC has a major problem with chattering phenomena, which can result in damage to actuators [14], [15]. In addition, for control rider-motorcycle systems, a simple model derived from a variant of the RIP system is used to control circular movement on tracks with variable radii. The RIP system is employed in various applications, e.g., aerospace vehicle control, position control, and robotics [16], [17]. The RIP system incorporates an arm that is driven by voltage and revolves horizontally, and the pendulum is attached to this and revolves along with a vertical position. In a RIP, the pendulum always moves in a plane perpendicular

The associate editor coordinating the review of this manuscript and approving it for publication was Xiaojie Su.

to that of the rotating arm. Issues related to ''nonlinearity, robustness, following up and tracking'' are demonstrated by the pendulum [18], [19], [20], [21]. The control of this system is essential and complex due to its two degrees of freedom and single control input. Thus, the pendulum has become the benchmark for various control techniques. In the literature, most control models are linear methods, and such methods are not suitable for controlling due to disturbances and nonlinearities. Among nonlinear methods, SMC is more robust and accurate. Therefore, a system is required to realize optimal gain parameter tuning.

Our primary contributions are summarized as follows.

- A control strategy that integrates a PID controller and SMC strategy is proposed to address the nonlinearity issues of underactuated RIP systems.
- In the proposed strategy, controller parameters are optimized using a modified Manhattan distance updated WOA (MMD-WOA).
- Response for sinusoidal input and its variation in Phase, amplitude and an error analysis is conducted to evaluate the performance of the proposed method compared to conventional models.

The remainder of this paper is organized as follows. Related work is summarized in Section II, and Section III describes the system model of the proposed PID-SMC optimization method using the MMD-WOA algorithm. Section IV describes the optimal tuning of the coefficients of controllers using the proposed MMD-WOA algorithm. Finally, the paper is concluded in Section V.

II. LITERATURE REVIEW

In 2017, a previous study [1] compared LQR performance in terms of the integral square error criterion for a step-change in pendulum angle. That study also performed uncertainty tests by adding loads to the end of the pendulum. The simulation results demonstrated that the proposed method generated better responses compared to conventional control strategies. In 2020, another study [2] introduced a grey wolf optimizer via particle swarm optimization (PSO) based on the adaptive constant method to tune the parameters of a variable structure adaptive fuzzy controller with reduced LQR (RLQR). Due to its high performance, grey wolf optimization can realize real-time implementation.

In 2017, a previous study [3] proposed the 2-loop fractional PID (2-Loop FPID) control method for a rotary type single IP to improve its potential. Here, a simple graphical tuning method was developed based on the frequency response to regulate the parameters of the 2-Loop FPID controller. In addition, dynamic PSO was employed to fine-tune the same parameters. In addition, saturation nonlinearity was compensated by integrating the back-calculation anti-windup method. They have investigated the 2-Loop FPID method in terms of robustness.

In 2019, a previous study [4] proposed an intelligently optimized self-tuning fractional-order control strategy for an IP to improve its attitude stabilization. In this strategy, the fractional-order proportional derivative controllers are employed to reduce deflections in its state trajectories. In addition, the system's immunity against exogenous disturbances was improved by dynamically adjusting the PD gains of each controller using piecewise nonlinear functions, which is accomplished at the end of each sampling interval. Here, the fractional-number power of the derivative operator and nonlinear gain-adjustment functions of each controller are selected using the PSO algorithm. The authors tested their model in the ''QNET Rotary Inverted Pendulum setup via 'hardware-in-the-loop experiments','' and the results have exhibited significant improvement in the ''error elimination capability, convergence-rate, transient recovery, and disturbance rejection capability.''

In 2020, another study [5] proposed a continuous fuzzy-based super-twisting stabilization algorithm (FBSTSA) to solve stability issues in underactuated RIP systems. Initially, a new sliding surface is introduced utilizing integrating a fully-actuated rotary arm and underactuated pendulum variables to resolve the under-actuation problem. The continuous FBSTSA is used to tune the control gains concerning the fuzzy rules. With the proposed FBSTSA, they demonstrated that the sliding variable can reach zero at a defined time limit, and then the closed-loop system state converges to zero asymptotically.

A previous study [6] projected an optimized interval type 2 fuzzy proportional derivative controller (IT2F-PDC) in series form for the RIP. Here, the IT2F-PDC parameters are optimized using a genetic algorithm (GA) and PSO. In addition, the goal of this study was to usher the pendulum to its equilibrium position. Experimental results demonstrated the potency and strength of GA-PSO-based controllers for RIPs by considering load disturbances, parameter variation, and noise effects.

In 2019, a previous study [7] applied a model-free backstepping (MFBS) control technique to study the control mechanism of a RIP. Then, the system model's ordinary representation was made using the MFBS technique, and it further estimated the unknown dynamics. The MFBS-based control design was compared to the LQR control invariant settings, and the results demonstrated that the performance of the proposed control system was good in terms of control performance.

In 2020, Reference [8] developed a fuzzy-based linear quadratic regulator (FLQR) and a FLQ Gaussian (FLQG) controller for a double link RIP (DLRIP) system to control the steadiness of the system. In this study, the FLQR and FLQG controllers were analyzed dynamically and compared to traditional LQR and LQG controllers. The authors compared control performance in terms of the time required for settling, peak overshoot, error in the steady-state and the overall root mean square errors (RMSE).

In 2021, [36] advocated a control law based on feedback linearization blended with PI controller that avoids the hectic task of finding a solution for partial differential equations for the pendulum process and the results are tested for step

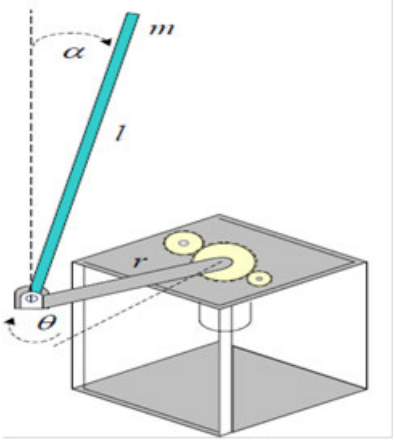

FIGURE 1. A rotary inverted pendulum setup.

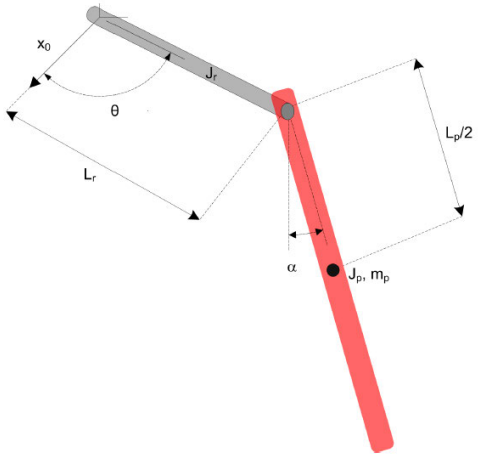

FIGURE 2. Parameters associated with rotary inverted pendulum setup.

response of the primary angles. Reference [37] presented an adaptive SMC for the position and Tracking control of Quadrotor UAV in the presence of Disturbance and is compared with the duo of PID and SMC and the outcomes are tested for step responses with square wave as input.

III. THE PROPOSED CONTROL STRATEGY

A. ROTARY INVERTED PENDULUM (RIP)

The system model of the RIP is displayed in Fig.1. It comprises a rotary cart base and a pendulum. At the center surface of the cart, the pendulum is pivoted which can revolve about the hinge in the alike perpendicular surface with a circular rail-like arrangement. The rotor arm angle, θ (in radians) and pendulum angle, α (in radians) and other parameters associated with the system are represented in Fig. 2. The total kinetic and potential energy of the system is found primarily to compute the Euler-Lagrangian derivatives to yield the Equations of Motion (EOM) of RIP. The resultant non-linear EOM of the RIP system is represented by (1) - (3),

$$\begin{bmatrix} J_p - m_p rl\cos\theta \\ -m_p rl\cos\theta J_r + J_p\sin^2\theta \end{bmatrix}\begin{bmatrix}\dot{\theta}\\ \dot{\alpha}\end{bmatrix} + \begin{bmatrix} -1/2 * J_p\dot{\alpha}\sin 2\theta - m_p gl\sin\theta \\ J_p\dot{\alpha}\dot{\theta}\sin 2\theta - m_p lr\dot{\theta}^2\sin\theta \end{bmatrix} = \begin{bmatrix}0\\ \tau\end{bmatrix} \tag{1}$$

$$\left[m_p L_r^2 + \frac{1}{4}m_p L_p^2 - \frac{1}{4}m_p L_p^2\cos(\alpha)^2 + J_r\right]\ddot{\theta} - \left[\frac{1}{2}m_p L_p L_r\cos(\alpha)\right]\ddot{\alpha} + \left[\frac{1}{2}m_p L_p^2\sin(\alpha)\cos(\alpha)\right]\dot{\theta}\dot{\alpha} + \left[\frac{1}{2}m_p L_p L_r\sin(\alpha)\right]\dot{\alpha}^2 = \tau - D_r\dot{\theta} \tag{2}$$

$$\left[\frac{1}{2}m_p L_p L_r\cos(\alpha)\right]\ddot{\theta} + \left[J_p + \frac{1}{4}m_p L_p^2\right]\ddot{\alpha} - \left[\frac{1}{4}m_p L_p^2\sin(\alpha)\cos(\alpha)\right]\dot{\theta}^2 + \left[\frac{1}{2}m_p L_p g\sin(\alpha) = -D_p\dot{\alpha}\right] \tag{3}$$

Here, g = 9.8 m/s^2 is the acceleration due to gravity, and τ is the applied torque. There is no friction within the cart and the rotary arm base or within the rotary arm and the pendulum. Thus, system's friction is assumed to be zero. Solving for acceleration terms and having defined the states of the system, the linearized state space model of the RIP is given by (4)-(6) [27], [28], [29].

$$\dot{X(t)} = Ax(t) + Bu(t)$$
$$Y(t) = Cx(t) \tag{4}$$

where

$$A = \frac{1}{J_T}\begin{bmatrix} 0 & 0 & J_T & 0 \\ 0 & 0 & 0 & J_T \\ 0 & \frac{1}{4}M_p^2 L_p^2 L_r g & -K_1 D_r & K_2 D_p \\ 0 & -\frac{1}{2}m_p L_p g(K_3) & \frac{1}{2}m_p L_p L_r D_r & -K_3 D_p \end{bmatrix} \tag{5}$$

$$B = \frac{1}{J_T}\begin{bmatrix}0\\0\\K_1\\-K_2\end{bmatrix}; C = \begin{bmatrix}1&0&0&0\\0&1&0&0\end{bmatrix} \tag{6}$$

where

$$K_1 = (J_p + \frac{1}{4}m_p L_p^2)$$
$$K_2 = \frac{1}{2}m_p L_p L_r$$
$$K_3 = (J_r + mpLr^2)$$

and the corresponding states and output (7) are defined to be

$$x = \begin{bmatrix}\theta & \alpha & \dot{\theta} & \dot{\alpha}\end{bmatrix}^T; y = \begin{bmatrix}\theta & \alpha\end{bmatrix}^T \tag{7}$$

where θ represents the angular measurements of rotor arm angle, (in radians) with respect to the base and α represents Pendulum angle, (in radians); $\dot{\theta}$ and $\dot{\alpha}$ are their corresponding velocities respectively. Table 1 enlists the values of the parameters used for the analysis. Thus, the main objective is to control the pendulum angle such that it tracks the position appropriately and comes to rest in a vertical position whereas

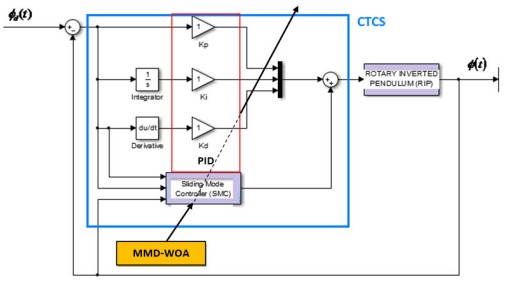

FIGURE 3. Congruently tuned control strategy.

the cart can have a minor shift with respect to origin [26]. The system matrix A and Input matrix B of RIP (8)-(9) is obtained using the parameter values enumerated in Table - 1 and is given by

$$A = \begin{bmatrix} 0 & 0 & 1 & 0 \\ 0 & 0 & 0 & 1 \\ 0 & 149.2751 & -0.0104 & 0 \\ 0 & 261.6091 & -0.0103 & 0 \end{bmatrix} \tag{8}$$

$$B = \begin{bmatrix} 0 & 0 & 49.7275 & 49.1493 \end{bmatrix}^T \tag{9}$$

and the Eigenvalues are computed to be in (10)

$$\begin{bmatrix} 0 & -16.1773 & 16.1714 & -0.0046 \end{bmatrix}^T \tag{10}$$

which indicated a presence of one pole in the right half of s-plane indicating the unstable nature of the system.

B. CONGRUENTLY TUNED CONTROL STRATEGY (CTCS)

The main aspiration of the control scheme is balancing the RIP, so that the pendulum always rests in an upright manner in its inverted position by controlling the position of the cart on the circular track rapidly and precisely. Fig.3 manifests the congruently tuned control strategy. The proposed strategy comprises a PID and SMC, which are used to control the RIP. The PID block comprises a proportional gain (Kp), an integral gain (Ki), and a derivative gain (Kd). In addition, a feedback signal from the pendulum monitors the error between the system output and the desired position. Then, the relevant error signal e(t) should be provided to the PID and SMC blocks, which are used to control the RIP and whose parameters are to be fine-tuned. The SMC controller, which has inputs, i.e., the error signal e(t), derivative error, and the feedback signal from the pendulum, helps reduce the chattering problem with adequate gain tuning. Thus, the output of the PID and SMC controller is finely tuned, coherent to the constraints of the pendulum system, and creates a controller domain where both the PID and SMC can coexist. The proposed CTCS combines the PID and SMC without conflict in consideration of constraint priorities.

Sliding mode control has been recorded to be a robust and impressive control methodology for the stabilization of underactuated nonlinear systems [34]. The strategy is based on characterizing exponentially stable (sliding) surfaces as a function of the system states and utilizing the Lyapunov theory to establish all closed-loop system trajectories reach the assured surfaces in finite time. Since the closed-loop system dynamics on the surfaces are exponentially stable, the system trajectories slide along the surfaces until they rise to the origin. The sliding mode control law designated for underactuated systems assorts the stabilization problem based on equilibrium. The sliding mode control law is determined with defined Lyapunov function for a underactuated two-degree-of-freedom nonlinear system, that guarantees exponential stability and the Lyapunov function also allows to predict the field of attraction on the sliding surface securing that all closed-loop system trajectories approaching this field will

TABLE 1. RIP parameters.

S.No.	Parameters with Units	Symbol	Numerical Values used
Motor			
1	Resistance, Ω	R_m	8.4
2	Current-torque, N-m/A	K_t	0.042
3	Back-emf Constant, V-s/rad	K_m	0.042
Rotary Arm			
4	Mass of the Rotary arm, Kg	m_r	0.095
5	Length of the Rotary arm, m	L_r	0.085
6	Moment of Inertia about Pivot (Rotary arm), Kgm^2	J_r	$5.71X10^{-5}$
7	Viscous Damping Coefficient (Rotary arm), N-m-s/rad	D_r	0.0015
Pendulum			
8	Mass of the Pendulum, Kg	m_p	0.024
9	Length of the Pendulum, m	L_p	0.129
10	Moment of Inertia about Pivot (Pendulum), Kgm^2	J_p	$3.3282X10^{-5}$
11	Viscous Damping Coefficient (Pendulum), N-m-s/rad	D_p	0.0005

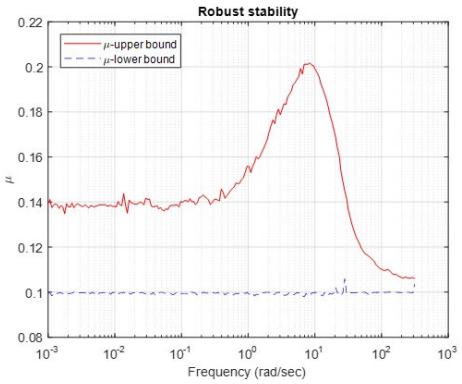

FIGURE 4. Robust stability analysis of SMC-PID controller.

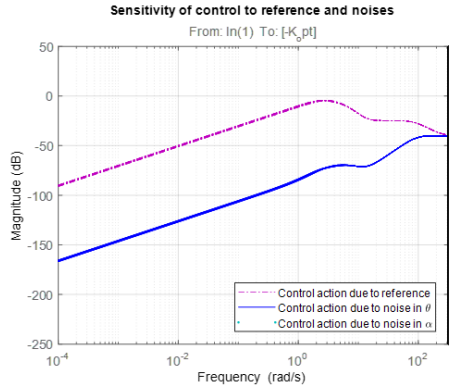

FIGURE 5. Magnitude response of sensitivity of control action due to input and noises in output.

concur exponentially to the origin while sliding along the surface.

The robust stability analysis is recorded to have a peak value of less than 1 and of value 0.2 for the SMC-PID controller. This result is shown in Figure 4 and Figure 5 displays the magnitude response of sensitivity of control action with respect to the reference and noise in the outputs of rotary inverted pendulum SMC-PID Controller that publishes to be in limited magnitudes at low frequencies with exclusive disparities for the controller scheme.

The feedback linearization for a class of non-linear system [34] in (11) is calculated as mentioned below:

$$\ddot{\phi} = g(\phi, t) + h(\phi, t)u_t \tag{11}$$

According to [31], the control input of PID (12) is defined as

$$u_{PID} = K_p e(t) + K_i \int e(t)dt + K_d \frac{d}{dt} e(t) \tag{12}$$

The sliding mode control is given by (13)-(14)

$$u_{SMC} = \frac{V - g(\phi, t)}{h(\phi, t)}$$

where

$$V = \ddot{\phi}_d(t) + c_1 e(t) + c_2 \dot{e}(t)$$

$$u_{SMC} = \frac{\ddot{\phi}(t) + c_1 e(t) + c_2 \dot{e}(t) - g(\phi, t)}{h(\phi, t)} \tag{13}$$

The overall combination of SMC and PID approach of the proposed controller is given by (14)

$$u_t = u_{SMC} + u_{PID}$$

$$u_t = \frac{\ddot{\phi}(t) + c_1 e(t) + c_2 \dot{e}(t) - g(\phi, t)}{h(\phi, t)} + K_p e(t) + K_i \int e(t)dt + K_d \frac{d}{dt} e(t) \tag{14}$$

C. OPTIMIZATION BASED PID-SMC CONTROLLER

Owing to its underactuated nature with the availability of one actuator for two degrees of freedom and the open-loop characteristics instability, designing of control strategy for RIP using PID controller is a quiet challenging task. The major problem in sliding mode control is chattering phenomena, because of its low control accuracy. Hence, a hybrid control of PID based SMC Controller with better performance is opted with adequate gain tuning to reduce the chattering. In order to achieve tuned gains, the parameters of PID controller namely, "proportional gain (K_p), Integral gain(K_i) and Derivative gain (K_d) and the coefficients (c_1)and (c_2)of SMC will be fine-tuned by a Modified Manhattan Distance Updated Whale Optimization Algorithm (MMD-WOA), obtained via improving the standard WOA. Thus, the MMD-WOA is presented to choose the prompt sliding surface coefficients and the gain parameters as well to minimize tracking error.

IV. OPTIMAL TUNING OF GAIN PARAMETERS AND SLIDING SURFACE COEFFICIENTS BY MMD-WOA

A. SOLUTION ENCODING AND OBJECTIVE FUNCTION

For precise error minimization, the presented work plans to tune the proportional, integral and derivative gain constraints (K_p,K_i,K_d) of PID controller and the coefficients (c_1,c_2) of the SMC, such that the error between tracking position and the desired position can be minimized. Thus, the defined function for the objective (OF) of the proposed methodology is specified in (15).Here, ($\phi_d(t)$)represents the desired position, ($\phi(t)$) represents the tracking position.

$$error = \phi_d(t) - \phi(t)$$
$$OF = Min(error) \tag{15}$$

B. MODIFIED MANHATTAN DISTANCE UPDATED WOA ALGORITHM

The whale optimization algorithm (WOA) is a comparably new meta-heuristic optimization approach [22] which is

inspirited by the bubble-net hunting of humpback whales. The implementation of WOA is uncomplicated and has meagre modifications in their parameters, that prints outperforming results when compared to particle swarm optimization (PSO), grey wolf optimizer (GWO), gravitational search algorithm, and so on. WOA has a good convergence rate, but the performance of WOA in finding the global optimal solution of an underactuated, non-linear, unstable process with multiple local optimal solutions is not ideal. In this work, a Modified Manhattan-Distance based whale optimization algorithm (MMD-WOA) algorithm is proposed, with four main enhancements: (1) Distance based position identification (2) Logarithmic based position updation to handle nonlinearities (3) Nonlinear fitness estimation design is introduced to balance the ratio of exploitation phase and exploration phase. (4) Random position clustering and shrinking encircling strategy is picked to disintegrate population into numbers of groups for bettering the diversity of population. Location based exploration phase are used to augment the search of prompt sliding surface co-efficients and gain parameters and also minimize error.

Modified Manhattan Distance Updated Whale Optimization Algorithm (MMD-WOA) is a novel meta-heuristic algorithm that is developed from the classical Whale Optimization Algorithm (WOA) [22] which is based on the Whale's behaviour while hunting the prey: It incorporates three main phases namely, ''Encircling prey, Bubble-net attacking model and Searching for prey''. Circling the prey: Naturally, the Whales are capable of identifying the prey's present location and they start to surround the prey. However, the location of the optimum solution (i.e., (K_p,K_i,K_d) and (c_1,c_2)) are not known in advance, so that the algorithm is used to find the solution which approaches the optimum one. As soon as the best agent is fixed, while the iteration repeats, the other agents will try to upgrade their locations with respect to the best agent.

$$D_s = |C_s X_s^*(t) - X_s(t)| \tag{16}$$

$$X_s(t+1) = w * w1 * (X_s(t) - A_s D_s) \tag{17}$$

Here, A_s and D_s are coefficient vectors (16), t refers the current iteration, X_s^* represents the position vector of acquired optimal solution and the position vector is represented as X_s the real value is indicated by ||, and represents the multiplication. The vector evaluation of A_s is based on the modified Manhattan distance as per (18) and hence it is called as MMD-WOA and C_s is formulated as per (19), in which r_s represents the random vector limited over the interval (0,1).

$$A_s = \frac{1}{N} \sum_{s=1}^{N} \frac{|X_s - X_s^*|}{|X_{max_s} - X_{min_s}|} \tag{18}$$

$$C_s = 2r_s \tag{19}$$

Bubble-net Attacking Model: The bubble-net behaviour of humpback whales comprises of 2 approaches. a. Shrinking Encircling model: From the current position of the optimal whale and the true position of the whale, a new position for whale can be fixed by assigning the values for A_s among (-1,1) randomly. b. Spiral Updating position: This phase calculates the distance among the whale location (X_s,Y_s) and prey location(X_s^*,Y_s^*) stated in (20), wherein h refers a fixed term that defines the logarithmic spiral form, f is a random number in $(-1,1)$ and $D_s = |X_s^*(t) - X_s(t)|$ indicates the distance among whale and prey.

$$X_s(t+1) = D_s e^{hf} \cos 2\pi f + X_s^*(t) \tag{20}$$

For modelling the concurrent behaviour, it is presumed that a chance of 50% is there to select among either ''the shrinking encircling mechanism or the spiral mode'' for the whale's location upgrade throughout optimization. So, the arithmetic modelling is explained in (21).

$$X_s(t+1) = \begin{cases} X_s^*(t) - A_s D_s if p_r < 0.5 \\ D_s e^{hf} \cos 2\pi f + X_s^*(t) if p_r \geq 0.5 \end{cases} \tag{21}$$

Prey Searching: In this phase, humpback whales search is randomly based on the location. Therefore, use of A_s with arbitrary values > 1 or < 1 will force the whale to relocate away from the whale which is a reference one. The randomly selected search agent is deployed to upgrade the location of the search agent within the global search. Now, mathematical model for the exploration phase (22)-(23) is given as

$$D_s = |C_s X_{sran} - X_s| \tag{22}$$

$$X_s(t+1) = w * (1 - w1) * X_{sran} - A_s D_s \tag{23}$$

where, X_{sran} indicates the random position vector selected among the present population. Fig.6 represents the flowchart structure of the proposed Modified Manhattan Distance Updated-WOA algorithm.

The algorithm was subjected to 30 iterations and the choice of controller parameters were suggested by the algorithm and as proportional gain (K_p) = 0 to 20, Integral gain(K_i) = 0 to 2 and Derivative gain (K_d) = 0 to 2 and the coefficients (c_1) and (c_2) of SMC to be from 0 to 5;

V. RESULTS AND DISCUSSIONS

The proposed PID-SMC controller for the RIP was executed in MATLAB/Simulink and analysis was done. The performance of Sliding Mode Controller (SMC), Fire Fly Algorithm (FFA) and Whale Optimization Algorithm (WOA) is compared with the proposed MMD-WOA to stabilize the tracking position of RIP for the upright position. $\phi_d(t)$. Finally, superposition of these actions constitutes the mechanism of the control strategy. Here, the performance of the SMC, FireFly algorithm (FFA), and WOA were compared to that of the proposed MMD-WOA in terms of stabilizing the

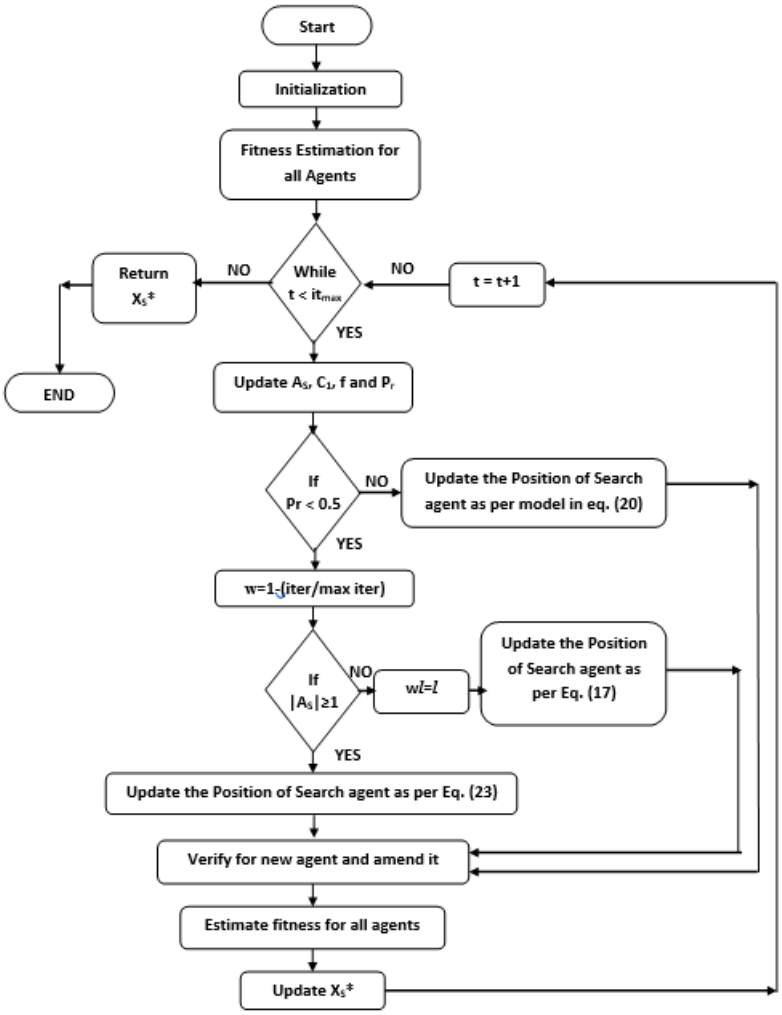

FIGURE 6. Flowchart of proposed MMD-WOA.

tracking position of a RIP in the upright position. The parameters of PID controller namely, proportional gain (Kp), Integral gain (Ki) and Derivative gain (Kd) is computed to be 15.9446,1.9406 and 1.6452 respectively and the coefficients (c_1) and (c_2) of SMC is 4.6210 and 4.1349 respectively.The MMD -WOA parameters A_s is chosen to be 1 and $w1$ to be 0.

The algorithm is iterated for a maximum of 30 times with ode 45 solver with variable-step type and enabling auto updation of step size to enable smooth conduction of analysis with sine wave input. Figure 7 show a Convergence curve of FFA, and WOA controllers compared to that of the proposed MMD-WOA,that ensures MMD-WOA responds rapidly to load variations with fewer tuning parameters and D_s the distance factor also acts as a limiting factor to prevent the values frequently leaving from search space leading to a quick exploration phase. Figure 8 compares different control techniques by analyzing the response, the control signal,

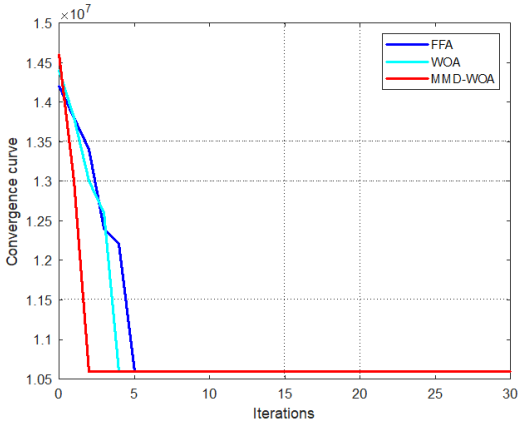

FIGURE 7. Convergence curve of optimization algorithms.

and the error signal based on the desired tracking position. Figure 8(a) shows the time response. As can be seen, tracking

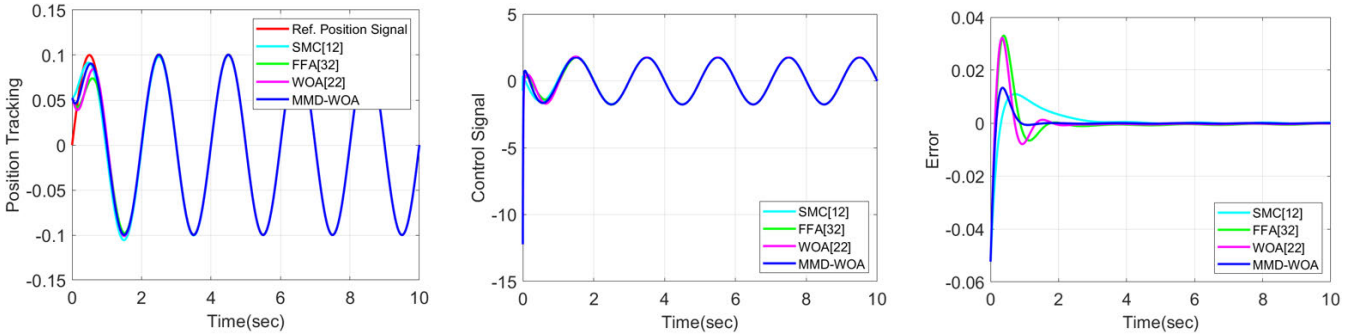

FIGURE 8. Performance analysis of proposed over traditional methods.

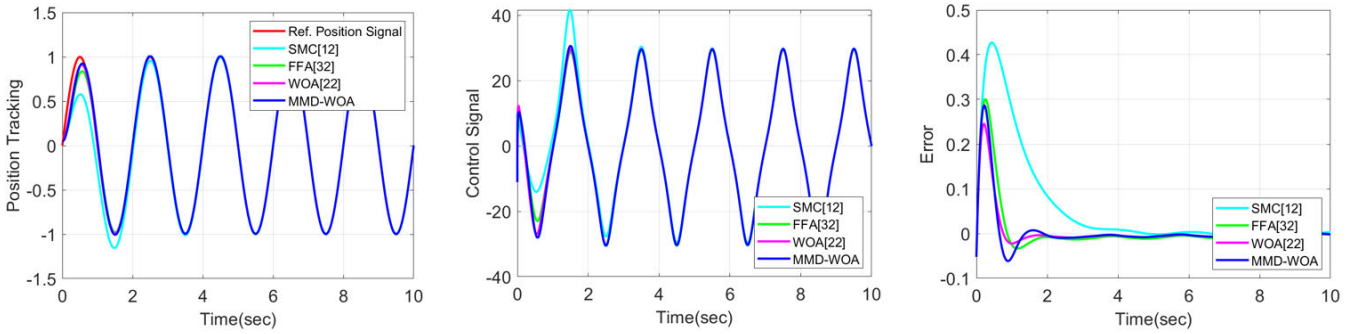

FIGURE 9. Case-1-performance analysis of proposed over traditional methods.

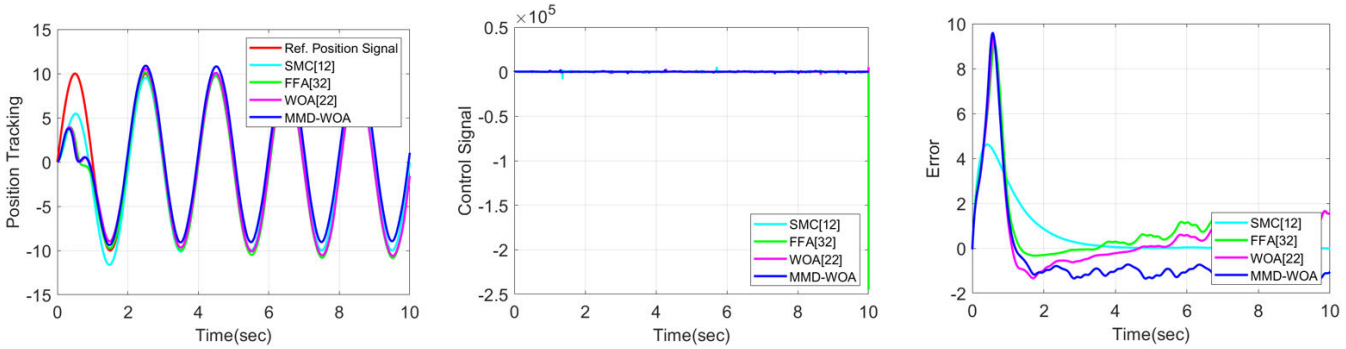

FIGURE 10. Case-2-performance analysis of proposed over traditional methods.

stability at the desired reference position is achieved after 1 s. Thus, the proposed MMD-WOA controller is much better compared to the conventional WOA. The stabilization times of the SMC and FFA are 1.8 s and 1.6 s, respectively. Figure 8(b) compares the control signal. As shown, the proposed strategy exhibits effortless control over that of classical approaches, and it is also clear that chattering is absent. Figure 8(c) shows the error signal. Here, the steady-state error at the desired reference position is taken as zero. After 0.5 s, the proposed MMD-WOA controller reaches the desired reference position faster than the compared controllers.

A. PERFORMANCE ANALYSIS

Figures 9 and 10 show performance analysis of SMC, FFA, and WOA controllers compared to that of the proposed MMD-WOA. Case-I and II results are based on the amplitude variation. Hence, the position of the desired tracking point changes to $\phi_d(t) = 1 \sin \pi t$ and $\phi_d(t) = 10 \sin \pi t$ respectively. Here, the amplitude of the desired reference position is set to 1 rad/sB2 and 10 rad/s2. In addition, the proposed controller reaches the desired reference position after 0.8 s and 3 s compared to the other controllers. Case III and IV are imprinted in Figures 11 and 12 respectively when the position of the desired tracking point changes to

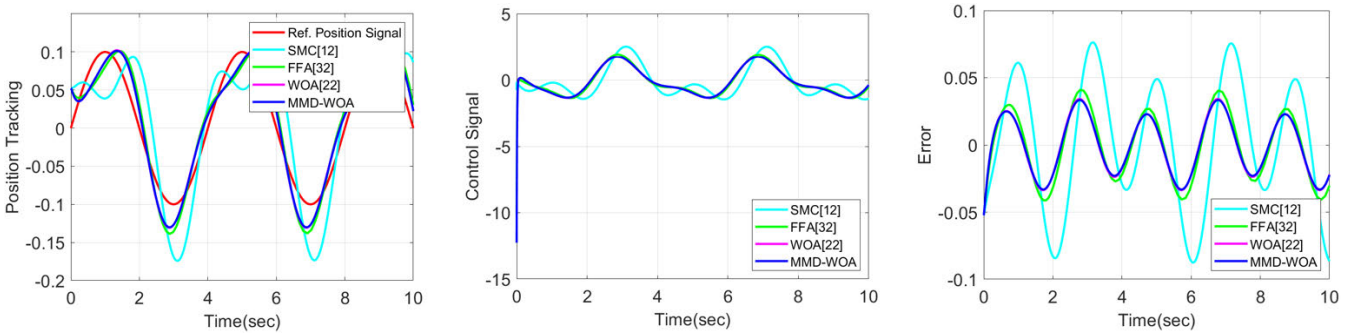

FIGURE 11. Case-3-performance analysis of proposed over traditional methods.

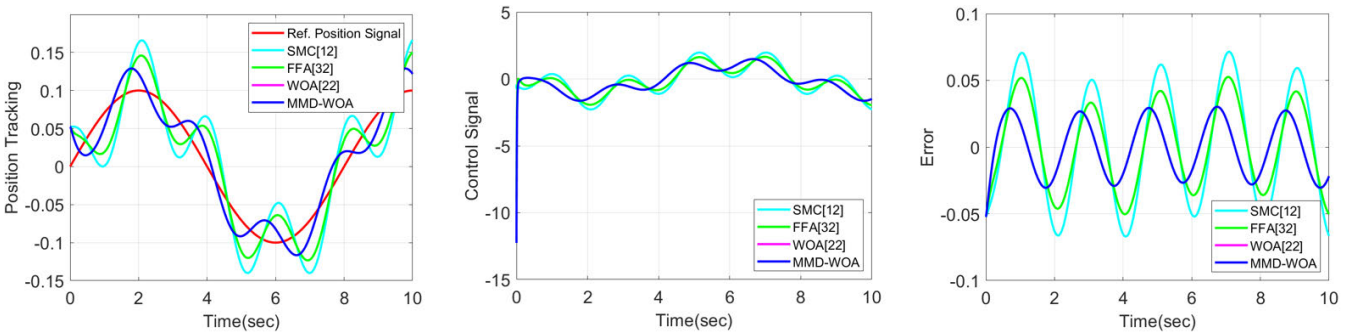

FIGURE 12. Case-4-performance analysis of proposed over traditional methods.

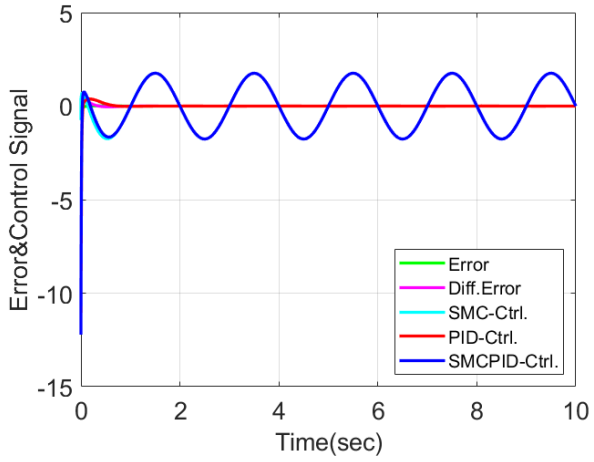

FIGURE 13. Error signal and control signal of controllers on discussion.

TABLE 2. Error performance analysis for proposed work.

	SMC [12]	FFA[32]	WOA[22]	MMD-WOA
MAE	0.0032143	0.012309	0.011737	0.0021036
MSE	8.5723×10^{-5}	0.00025176	0.00023634	7.2198×10^{-5}
RMSE	0.0092587	0.015867	0.015373	0.0084969

$\phi_d(t) = 0.1 \sin \frac{\pi}{2} t$ and $\phi_d(t) = 0.1 \sin \frac{\pi}{4} t$ based on the frequency variation. The stability of the reference position tracking frequency completes one cycle after $\pi/2$ rad/sec and $\pi/4$ rad/sec. Note that the frequency of the proposed controller is not as accurate as the reference controller; however, the proposed MMD-WOA controller is much better than that of the other controllers. Thus, optimized gain can be achieved by controlling the parameters, and the desired control signal and error signal output are obtained. Figure 13

TABLE 3. Error performance analysis for case-1.

	SMC [12]	FFA[32]	WOA[22]	MMD-WOA
MAE	0.057203	0.12427	0.1666	0.018147
MSE	0.015497	0.022284	0.048381	0.002449
RMSE	0.12449	0.14928	0.21996	0.049488

TABLE 4. Error performance analysis for case-2.

	SMC [12]	FFA[32]	WOA[22]	MMD-WOA
MAE	0.63003	4.5602	7.3783	1.4113
MSE	1.8261	32.548	81.676	4.7345
RMSE	1.3513	5.7051	9.0375	2.1759

TABLE 5. Error performance analysis for case-3.

	SMC [12]	FFA[32]	WOA[22]	MMD-WOA
MAE	0.040647	0.062601	0.019907	0.019706
MSE	0.0022068	0.006234	0.0005143	0.000504
RMSE	0.046976	0.078956	0.022451	0.022451

TABLE 6. Error performance analysis for case-4.

	SMC [12]	FFA[32]	WOA[22]	MMD-WOA
MAE	0.039271	0.028712	0.019854	0.019881
MSE	0.0019262	0.001048	0.0005051	0.0005064
RMSE	0.043889	0.032373	0.022475	0.022505

shows the corresponding error signal and control signal for various controllers.

B. ANALYSIS ON ERROR MEASURES

The analyses of the presented model by considering the error metrics for the different cases are revealed from the tabulated values. From table 2, the MAE performance of the proposed MMD-WOA scheme is 34.55% better than SMC, 82.91% better than FFA and 82.07% better than WOA schemes. Also, MSE of the suggested MMD-WOA model is 1.9% better than WOA-PIDSMC scheme. Moreover, the RMSE measure of the presented MMD-WOA technique is 48.72% superior to SMC, 30.48% better than FFA and 0.13% better than WOA.

VI. CONCLUSION

This paper has proposed the CTCS with a modified Manhattan distance updated WOA for rotary inverted pendulums. A performance analysis demonstrated that the proposed strategy outperformed SMC, the FireFly algorithm, and the conventional WOA in terms of error reduction, as shown in Tables 2 to 6. In addition, the proposed control strategy exhibits less chattering, higher precision, and no oscillation. The gain tuning of the proposed strategy realizes excellent position tracking and minimal control effort (Figure 7), and for different cases, analysis are carried out in terms of amplitude and phase angle variations that are obvious in Figures 8–11. Thus, the simulation and error performance results suggest that the optimal tuning of the gain parameters obtained by the proposed strategy can improve reliability and minimize errors by enhancing the quality of the result. As a result, it is believed that the proposed control strategy would be highly effective for the control of underactuated, unstable, and non-minimum phase systems.

REFERENCES

[1] I. Paredes, M. Sarzosa, M. Herrera, P. Leica, and O. Camacho, "Optimal-robust controller for Furuta pendulum based on linear model," in *Proc. IEEE 2nd Ecuador Tech. Chapters Meeting (ETCM)*, Oct. 2017, pp. 1–6, doi: 10.1109/ETCM.2017.8247510.

[2] M. A. Ebrahim, M. E. Mousa, E. M. Said, M. M. Zaky, and S. A. Kotb, "Optimal design of hybrid optimization technique for balancing inverted pendulum system," *WSEAS Trans. Syst.*, vol. 19, pp. 138–148, Jun. 2020, doi: 10.37394/23202.2020.19.19.

[3] P. Dwivedi, S. Pandey, and A. S. Junghare, "Stabilization of unstable equilibrium point of rotary inverted pendulum using fractional controller," *J. Franklin Inst.*, vol. 354, no. 17, pp. 7732–7766, Nov. 2017, doi: 10.1016/j.jfranklin.2017.09.013.

[4] O. Saleem and K. Mahmood-Ul-Hasan, "Indirect adaptive state-feedback control of rotary inverted pendulum using self-mutating hyperbolic-functions for online cost variation," *IEEE Access*, vol. 8, pp. 91236–91247, 2020, doi: 10.1109/ACCESS.2020.2994830.

[5] N. P. Nguyen, H. Oh, Y. Kim, J. Moon, J. Yang, and W.-H. Chen, "Fuzzy-based super-twisting sliding mode stabilization control for under-actuated rotary inverted pendulum systems," *IEEE Access*, vol. 8, pp. 185079–185092, 2020, doi: 10.1109/ACCESS.2020.3029095.

[6] M. F. Hamza, H. J. Yap, and I. A. Choudhury, "Genetic algorithm and particle swarm optimization based cascade interval type 2 fuzzy PD controller for rotary inverted pendulum system," *Math. Problems Eng.*, vol. 2015, pp. 1–15, Jul. 2015, doi: 10.1155/2015/695965.

[7] J. Huang, T. Zhang, Y. Fan, and J.-Q. Sun, "Control of rotary inverted pendulum using model-free backstepping technique," *IEEE Access*, vol. 7, pp. 96965–96973, 2019, doi: 10.1109/ACCESS.2019.2930220.

[8] Z. B. Hazem, M. J. Fotuhi, and Z. Bingul, "Development of a fuzzy-LQR and fuzzy-LQG stability control for a double link rotary inverted pendulum," *J. Franklin Inst.*, vol. 357, no. 15, pp. 10529–10556, Oct. 2020, doi: 10.1016/j.jfranklin.2020.08.030.

[9] X. Yang and X. Zheng, "Swing-up and stabilization control design for an underactuated rotary inverted pendulum system: Theory and experiments," *IEEE Trans. Ind. Electron.*, vol. 65, no. 9, pp. 7229–7238, Sep. 2018, doi: 10.1109/TIE.2018.2793214.

[10] Z. B. Hazem, M. J. Fotuhi, and Z. Bingul, "A comparative study of the joint neuro-fuzzy friction models for a triple link rotary inverted pendulum," *IEEE Access*, vol. 8, pp. 49066–49078, 2020, doi: 10.1109/ACCESS.2020.2978025.

[11] J.-B. Kim, H.-K. Lim, C.-M. Kim, M.-S. Kim, Y.-G. Hong, and Y.-H. Han, "Imitation reinforcement learning-based remote rotary inverted pendulum control in OpenFlow network," *IEEE Access*, vol. 7, pp. 36682–36690, 2019, doi: 10.1109/ACCESS.2019.2905621.

[12] R. J. Wai, M. A. Kuo, and J. D. Lee, "Design of cascade adaptive fuzzy sliding-mode control for nonlinear two-axis inverted-pendulum servomechanism," *IEEE Trans. Fuzzy Syst.*, vol. 16, no. 5, pp. 1232–1244, Oct. 2008, doi: 10.1109/TFUZZ.2008.924277.

[13] M. S. Park and D. Chwa, "Swing-up and stabilization control of inverted-pendulum systems via coupled sliding-mode control method," *IEEE Trans. Ind. Electron.*, vol. 56, no. 9, pp. 3541–3555, Sep. 2009, doi: 10.1109/TIE.2009.2012452.

[14] J. Huang, M. Zhang, S. Ri, C. Xiong, Z. Li, and Y. Kang, "High-order disturbance-observer-based sliding mode control for mobile wheeled inverted pendulum systems," *IEEE Trans. Ind. Electron.*, vol. 67, no. 3, pp. 2030–2041, Mar. 2020, doi: 10.1109/TIE.2019.2903778.

[15] J. Huang, Z.-H. Guan, T. Matsuno, T. Fukuda, and K. Sekiyama, "Sliding-mode velocity control of mobile-wheeled inverted-pendulum systems," *IEEE Trans. Robot.*, vol. 26, no. 4, pp. 750–758, Aug. 2010, doi: 10.1109/TRO.2010.2053732.

[16] J. Tian, J. Ding, Y. Tai, and Z. Ma, "Control of different-axis two-wheeled self-balancing vehicles," *IEEE Access*, vol. 8, pp. 158839–158851, 2020, doi: 10.1109/ACCESS.2020.3019538.

[17] S. Hwang and H. S. Kim, "Extended disturbance observer-based integral sliding mode control for nonlinear system via T–S fuzzy model," *IEEE Access*, vol. 8, pp. 116090–116105, 2020, doi: 10.1109/ACCESS.2020.3004241.

[18] M. Patil, B. Bandyopadhyay, A. Chalanga, and H. Arya, "Output tracking of nonminimum-phase systems via reduced-order sliding-mode design," *IEEE/ASME Trans. Mechatronics*, vol. 23, no. 4, pp. 1981–1992, Aug. 2018, doi: 10.1109/TMECH.2018.2836320.

[19] P. Dwivedi, S. Pandey, and A. S. Junghare, "Robust and novel two degree of freedom fractional controller based on two-loop topology for inverted pendulum," *ISA Trans.*, vol. 75, pp. 189–206, Apr. 2018, doi: 10.1016/j.isatra.2018.01.028.

[20] G. Pujol-Vazquez, L. Acho, S. Mobayen, A. Nápoles, and V. Pérez, "Rotary inverted pendulum with magnetically external perturbations as a source of the pendulum's base navigation commands," *J. Franklin Inst.*, vol. 355, no. 10, pp. 4077–4096, Jul. 2018, doi: 10.1016/j.jfranklin.2018.03.013.

[21] M. F. Hamza, H. J. Yap, I. A. Choudhury, A. I. Isa, A. Y. Zimit, and T. Kumbasar, "Current development on using rotary inverted pendulum as a benchmark for testing linear and nonlinear control algorithms," *Mech. Syst. Signal Process.*, vol. 116, pp. 347–369, Feb. 2019, doi: 10.1016/j.ymssp.2018.06.054.

[22] S. Mirjalili and A. Lewis, "The whale optimization algorithm," *Adv. Eng. Softw.*, vol. 95, pp. 51–67, May 2019, doi: 10.1016/j.advengsoft.2016.01.008.

[23] M. R. Tanweer, S. Suresh, and N. Sundararajan, "Self regulating particle swarm optimization algorithm," *Inf. Sci.*, vol. 294, pp. 182–202, Feb. 2015, doi: 10.1016/j.ins.2014.09.053.

[24] P. Ordaz and A. Poznyak, "Adaptive-robust stabilization of the Furuta's pendulum via attractive ellipsoid method," *J. Dyn. Syst. Meas. Control*, vol. 138, Mar. 2015, Art. no. 021005, doi: 10.1115/1.4032130.
[25] P. D. Mandic, M. P. Lazarevic, and T. B. Sekara, "D-decomposition technique for stabilization of Furuta pendulum: Fractional approach," *Bull. Polish Acad. Sci. Tech. Sci.*, vol. 64, no. 1, pp. 189–196, Mar. 2016, doi: 10.1515/bpasts-2016-0021.
[26] Z.-M. Yeh and K.-H. Li, "A systematic approach for designing multistage fuzzy control systems," *Fuzzy Sets Syst.*, vol. 143, no. 2, pp. 251–273, 2004, doi: https://doi.org/10.1016/S0165-0114(03)00203-3.
[27] Y. Becerikli and B. K. Celik, "Fuzzy control of inverted pendulum and concept of stability using Java application," *Math. Comput. Model.*, vol. 46, nos. 1–2, pp. 24–37, Jul. 2007, doi: 10.1016/j.mcm.2006.12.004.
[28] L.-X. Wang, *A Course in Fuzzy Systems and Control*. Upper Saddle River, NJ, USA: Prentice-Hall, 1996.
[29] M. Margaliot and G. Langholz, "A new approach to fuzzy modeling and control of discrete-time systems," *IEEE Trans. Fuzzy Syst.*, vol. 11, no. 4, pp. 486–494, Aug. 2003, doi: 10.1109/TFUZZ.2003.814836.
[30] J. Yi and N. Yubazaki, "Stabilization fuzzy control of inverted pendulum systems," *Artif. Intell. Eng.*, vol. 14, no. 2, pp. 153–163, Apr. 2000, doi: 10.1016/S0954-1810(00)00007-8.
[31] A. N. K. Nasir, R. Ismail, and M. A. Ahmad, "Performance comparison between sliding mode control (SMC) and PD-PID controllers for a nonlinear inverted pendulum system," *World Acad. Sci., Eng. Technol.*, vol. 71, pp. 400–405, Oct. 2010.
[32] A. H. Gandomi, X-S. Yang, S. Talatahari, and A. H. Alavi, "Firefly algorithm with chaos," *Commun. Nonlinear Sci. Numer. Simul.*, vol. 18, no. 1, pp. 89–98, Jan. 2013, doi: 10.1016/j.cnsns.2012.06.009.
[33] H. E. Mollabashi and A. H. Mazinan, "Incremental SMC-based CNF control strategy considering magnetic ball suspension and inverted pendulum systems through cuckoo search-genetic optimization algorithm," *Complex Intell. Syst.*, vol. 5, no. 3, pp. 353–362, Oct. 2019, doi: 10.1007/s40747-019-0097-0.
[34] A. E. Taha, M. Rahmat, J. Mu'azu, and M. Musa, "Feedback linearization and sliding mode control design for quadrotor's attitude and altitude," in *Proc. 1st Int. Conf. Mechatronics, Automat. Cyber-Phys. Comput. Syst.*, Mar. 2019, pp. 7–8.
[35] V. Utkin, "Variable structure systems with sliding modes," *IEEE Trans. Autom. Control*, vol. AC-22, no. 2, pp. 212–222, Apr. 1977, doi: 10.1109/TAC.1977.1101446.
[36] B. Salamat and A. M. Tonello, "A swash mass pendulum with passivity-based control," *IEEE Robot. Autom. Lett.*, vol. 6, no. 1, pp. 199–206, Jan. 2021, doi: 10.1109/LRA.2020.3037861.
[37] O. Mofid, S. Mobayen, and W.-K. Wong, "Adaptive terminal sliding mode control for attitude and position tracking control of quadrotor UAVs in the existence of external disturbance," *IEEE Access*, vol. 9, pp. 3428–3440, 2021, doi: 10.1109/ACCESS.2020.3047659.

ARULMOZHI NAGARAJAN (Member, IEEE) received the B.E. degree in electronics and instrumentation engineering from Bharathidasan University, in 2003, the M.Tech. degree in control system and instrumentation engineering from SASTRA University, in 2005, and the Ph.D. degree from Anna University Regional Campus, Coimbatore, India. She is currently an Assistant Professor (Senior Grade) with the Department of Electronics and Instrumentation Engineering, Government College of Technology, Coimbatore. She is also a MathWorks Certified MATLAB Associate. Her research interests include control systems, system identification, and H-infinity control.

ARULDOSS ALBERT VICTOIRE (Member, IEEE) received the B.Tech. degree from Pondicherry University, Puducherry, India, the M.E. degree from Madurai Kamaraj University, Madurai, India, and the Ph.D. degree from Anna University, Chennai, India, all in electrical engineering. He is currently an Associate Professor of electrical and electronics engineering with Anna University Regional Campus, Coimbatore, India. His research interests include developing hybrid intelligent optimization algorithms applied in power system operation and control, cyber-physical power systems, machine learning, and artificial intelligence.